



Original Article

Microstructure and Electrical Properties of Low-temperature Solution-processed Sol-gel KNN Thin Films

Vu Thu Hien^{1,*}, Nguyen Thi Minh Phuong^{1,2}

¹*International Training Institute for Materials Science (ITIMS),
Hanoi University of Science and Technology, 1 Dai Co Viet, Hanoi, Vietnam*

²*College of Industry and Trade, 1, Chua Cam, Trung Nhi, Phuc Yen, Vinh Phuc, Vietnam*

Received 04 February 2020

Revised 09 April 2020; Accepted 24 April 2020

Abstract: We report on an environmentally friendly and versatile chemical solution deposition route to $K_{0.5}Na_{0.5}NbO_3$ (KNN) thin films. The excess amounts of K and Na in KNN precursor solutions was found to be strong influence on perovskite KNN single-phase thin films. It was revealed from Raman spectroscopic analysis data that a change in scattering mode was observed for the KNN thin films fabricated under various processing conditions. This change was due to the chemical composition fluctuation of K and Na in the KNN thin films during heat treatment. The leakage current and ferroelectric properties of the thin films were strongly affected by the excess amounts of K and Na as well. KNN thin films with 20 mol% excess K and Na exhibited a leaky ferroelectric polarization–electric field (P–E) hysteresis. Leakage current density of the film was 3.85×10^{-8} A/cm² at applied field of -60 kV/cm.

Keywords: Lead-free KNN thin film, chemical solution deposition, microstructure, ferroelectricity.

1. Introduction

Lead-free alkaline niobate ferroelectrics [(Na_xK_{1-x})NbO₃, (KNN)] have attracted considerable attention due to their simple perovskite structure, high Curie temperature and very friendly with environment [1]. KNN, actually, is a solid solution of ferroelectric KNbO₃ (KN) and antiferroelectric NaNbO₃ (NN). At the compositions in the vicinity of morphotropic phase boundary MPB ($x = 0.5$), KNN has an orthorhombic phase at room temperature, and shows enhanced piezoelectric and ferroelectric properties [2]. Therefore, it makes them suitable for many applications [3–5]. In recent years, the demand for KNN material in the form of thin film has increased for the development of

*Corresponding author.

Email address: hien.vuthu@hust.edu.vn/ hienvt@itims.edu.vn

<https://doi.org/10.25073/2588-1124/vnumap.4460>

integrated devices, which require increasing miniaturization and integration [6]. However, the fabrication of dense alkaline niobate thin films is difficult because the alkaline elements volatilize during sintering process. This makes difficulty in obtaining saturated P–E hysteresis loops which results from high leakage current at high electric field. Therefore, proper excesses of K and Na play a key role in obtaining stoichiometric KNN thin films with high ferroelectric and piezoelectric properties. Recently, Soderlind *et al.*[7], Tanaka *et al.*[8], and Nakashima *et al.*[9] attempted to fabricate KNN thin films with a stoichiometric composition using a chemical solution deposition (CSD) method. However, the piezoelectric/ferroelectric properties of these thin films have not been fully characterized yet. In addition, KNN thin films containing alkaline excess by the sol–gel process are few and their electrical properties are needed to study further in order to clarify the characteristics for application in device.

In this study, KNN thin films were fabricated from 20 mol% (Na,K)-excess precursor solutions by the sol–gel process. The selected composition with 20 mol% (Na,K)-excess for obtaining high quality KNN thin films bases on the recent reports in [10]. The effect of starting A site ion (K and Na) composition in a precursor solution on the crystallographic structure, the surface morphology, and the electrical properties of the resultant KNN thin films was examined to realize novel, lead-free, piezoelectric thin films.

2. Experimental Section

Sodium acetate (CH_3COONa , 98%, Merck), potassium acetate (CH_3COOK , 99%, Merck), and niobium penta-ethoxide ($\text{Nb}(\text{C}_2\text{H}_5\text{O})_5$, 99.95%, Sigma Aldrich), 2-methoxy ethanol (2-MOE), and acetylacetone ($\text{CH}_3\text{COCH}_2\text{COCH}_3$) were used as the starting chemicals, solvent, and chelating agent, respectively to produce KNN precursor solutions. In order to compensate for the loss of alkaline metals during thermal processing, 20 mol% excess of the alkaline precursor was added to the KNN precursor solutions. The final concentration of KNN solution was adjusted to approximately 0.25 M. To obtain KNN thin films, the precursor solutions were spin-coated onto Pt/Ti/SiO₂/Si(100) substrates with the rate of 3000 rpm for 30 s. The wet films were dried at 150 °C for 5 min, subsequently, the dried gel films were increased to 300 °C for 10 min and then heated at 450 °C for 5 min using a tube furnace (TF55030C, Linberg/Blue M). These steps were repeated 6 to 10 times to achieve a desired thickness of the film. These films were annealed at 650-700 °C for 30 min in the ambient condition with a heating rate of 10 °C /min. The thickness of the annealed KNN films were about 595 nm.

The crystallographic information on the KNN film was established by using the XRD method (XRD; Philips X'pert). The surface morphology and thickness of the KNN films were evaluated by Field emission scanning electron microscopy (HELIOS 650, FIB-SEM, USA). The Raman measurements were conducted at room temperature in a Renishaw inVia confocal micro-Raman spectrometer, with an excitation wavelength of 532 nm provided by a He-Cd laser with a power of 4.85 mW focused on samples with magnification x50. To characterize of the electrical and ferroelectric properties, platinum electrodes (~ 100 nm thick) were sputtered on the surface of the film using a Cr-mask and lift-off lithography to form metal–insulator–metal (MIM) capacitors. Pad sizes of 9×10^{-4} , 36×10^{-4} , 1, 2.25, and 4 mm² were produced. Leakage currents were measured using a Keithley 4200-SCS instrument (Tektronic, USA) with a detection limit of 50 fA. The P–E hysteresis loops were measured using a TF-2000E analyzer (aixACCT Systems, Germany). All the measurements were performed at room temperature.

3. Results and Discussion

The deposited thin films were homogeneous with constant thickness and no cracks or defects were observed by eye. Hence a successful sol-gel route to KNN thin films was developed where the thickness of the film is easy to control by a number of spin-coated layers.

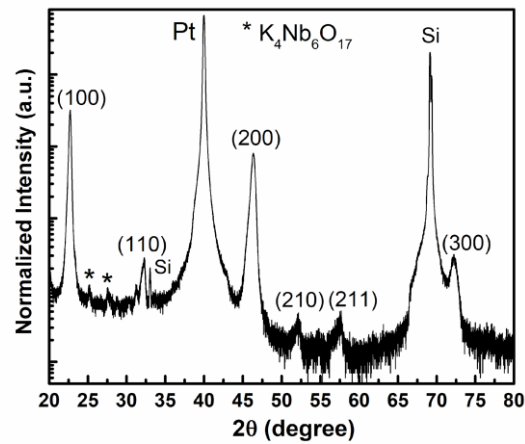


Figure 1. XRD pattern of the KNN thin film with 20 mol% excess of K and Na annealed at 650 °C/ 30 min in the air. The Miller indices of the main phase peaks and the peak positions of Pt electrode and Si substrate as reference are indicated.

The XRD patterns of KNN thin films with 20 mol% excess of K and Na annealed at 650 °C, are shown in Figure 1. The patterns demonstrated the presence of sharp Bragg reflections of KNN films along with the featured peaks of Pt electrode and Si substrate. The pseudo-cubic (100), (110) and (200) reflections of KNN are clearly shown, and the relative intensity of the pseudo-cubic (100) and (110) reflections demonstrate a substantial texturing of the sample. The (110)/(100) intensity ratio of the KNN film is approximately 0.009, as compared to the ratio of 1.05 for KNN powders in our case (not shown here). Besides perovskite phases, the XRD spectrum of the KNN film also consists of a small amount of $K_4Nb_6O_{17}$ –JCPDS 01-076-0977 secondary phases (denoted by * in the Figure 1), which have lower alkaline-to-niobium ratios 1:1.5 as compared to 1:1. The origin of the formation of these phases is attributed to the high volatilization of alkaline ions during the heat treatment and leading to an excess of Nb_2O_5 in the films [9–13]. Tanaka *et al.* reported that sodium-free secondary phases such as the $K_4Nb_6O_{17}$ can be formed easily because the volatilization rate of Na_2O is higher than that of K_2O which results to the split of $2\theta \sim 45.3^\circ$ in the XRD pattern of $KNbO_3$ powder fabricated by chemical process [9]. However, too much excess alkaline remained in the film will lead to the formation of secondary phase. We considered that secondary phases in the KNN film with 20% excess of alkaline in this case could be due to the surplus alkaline ions. Similar results are also reported by Kim *et al.* for KNN-30% thin films [14]. They found that the ratio of $(K + Na)/Nb$ of the KNN-30 thin film was 1.08, which meant that around 8 mol% alkaline ions remained in the KNN thin films.

Figure 2 presents SEM images of the surface and cross-sectional morphologies of KNN thin films heat-treated at 650 °C for 30 min on Pt/Ti/SiO₂/Si substrates. These images showed the surface of cohesions, which composed of the primary grains. The grain size of the film was estimated about $58 \div 274$ nm and surrounding the grains are distributed by small and dark pores. The causes of the morphology was attributed to be the vacancy or the secondary phases because the volatilization of alkaline ions suppressed grain growth [10]. An increase of annealing temperature may allow the coalescence of those small grains and assist to remove holes. The coalescence also leads to increase size of the intergranular porosity. Surface mappings were, then, confirmed by cross-sectional analysis shown in the insert image. As we can see, the out-of-plane grain sizes and morphologies are approximately the

same than the top surface: the grains are granular and mixed with voids. The total thickness of the film is *ca.* 595 nm for 10 coating layers, which turns out 59.5 nm per coating layer.

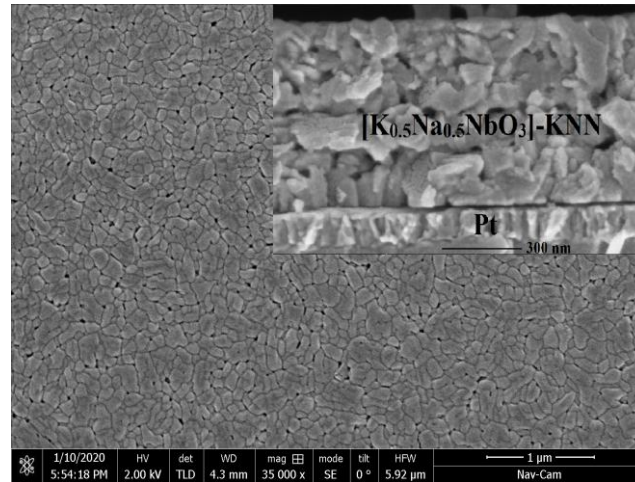


Figure 2. SEM images of the top surface and cross-section of spin-coated KNN thin films (the insert image).

In order to study the microstructures changes of KNN thin films with processing conditions, we performed Raman scattering measurements because the compositional fluctuation of alkali ions in the KNN structure can be assumed from the characteristic scattering position change. Typical room temperature Raman spectra of KNN thin films with 20% alkaline excess and annealing at 650 and 700 °C is depicted in Figure 3. The profiles in Figure 3 are consistent with those of KNN ceramics [15, 16] and thin films [14, 17] reported in the literatures. According to their theoretical analysis, a KNN crystal belonging the space group of $Amm^2 - C^{14}_{2v}$ has Raman active optical modes of $4A_1 + 4B_1 + 3B_2 + A_2$. The observed vibrations can be separated into external modes related to cations and internal modes of coordination polyhedra. Among the full Raman active mode of KNN, ν_1 , ν_2 , and ν_3 are stretching modes and ν_4 , ν_5 , and ν_6 are bending modes of the NbO_6 octahedra.

Table 1. Vibration wavenumber changes of ν_1 , ν_5 , ν_6 and $\nu_1 + \nu_5$ of KNN thin films in the term of annealing temperatures.

	ν_1/cm^{-1}	ν_5/cm^{-1}	ν_6/cm^{-1}	$\nu_1 + \nu_5/\text{cm}^{-1}$
KNN, 650 °C	613	244	191	845
KNN, 700 °C	620	260	190	846

We observed a spectrum change in the wavenumber region less than 200 cm^{-1} , and the modes around 600 , and 850 cm^{-1} . Table 1 summarizes Raman spectra of the KNN films and the peak positions of ν_1 , ν_5 , ν_6 and $\nu_1 + \nu_5$ modes in term of annealing temperature. A rather weak but still distinguishable shoulder at 191 cm^{-1} (ν_6) confirmed by Kakimoto *et al.* and Kim *et al.*, is assigned to the translation modes of Na^+/K^+ and K^+ cations versus the NbO_6 octahedra, respectively [14, 16]. The other internal vibrational modes [ν_1 , ν_2 , ν_3 , ν_4 , ν_5 , $\nu_1 + \nu_5$] of NbO_6 octahedra appear in a wide range from 200 to 900 cm^{-1} . In particular, ν_1 (613 cm^{-1}) and ν_5 (244 cm^{-1}) are detected as relatively strong scatterings and changed most drastically in KNN films with annealing temperature.

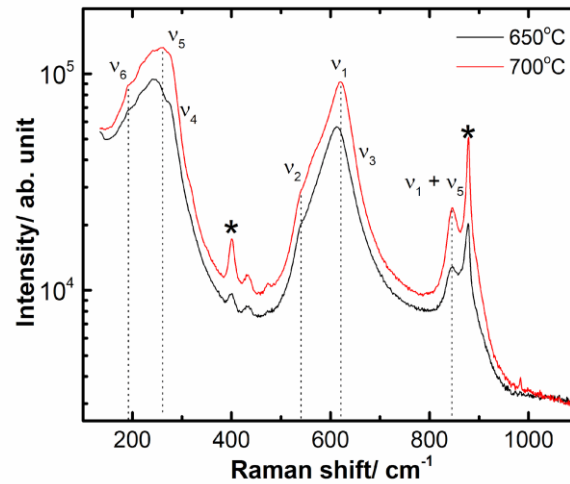


Figure 3. Room temperature Raman spectra of KNN thin films annealed at 650 and 700 °C.

The peak shift to a higher wavenumber side ($613 \rightarrow 620 \text{ cm}^{-1}$) as the temperature increased, is due to an increase in binding strength caused by the shortening of the distance between Nb^{5+} and its coordinated oxygens, resulting from the distortion of O–Nb–O angles. The same appearance is observed in the ν_5 bending mode as well. This shift usually occurs when the crystallinity becomes better and the A-site in the ABO_3 crystal structure is changed. The internal vibrational mode of $\nu_1 + \nu_5$ shows the coupled peak instead of unique single wavenumber. This coupled mode are reported by Kim *et al.* for the KNN-0% and KNN-30% films [14] and attributed to the highly distorted NbO_6 units caused by the deficiencies and redundancies of alkaline ions in the perovskite units. In this case of KNN-20% films $\nu_1 + \nu_5$ mode is located at around 845 and 878 cm^{-1} . These Raman modes are nearly similar to those location and intensity of $\text{K}_4\text{Nb}_6\text{O}_{17}$ [18]. As shown in Figure 1, the XRD pattern included tungsten bronze structures such as $\text{K}_4\text{Nb}_6\text{O}_{17}$ phases. Therefore, two distinct peaks in the $\nu_1 + \nu_5$ mode of the KNN film are influenced by the $\text{K}_4\text{Nb}_6\text{O}_{17}$ secondary phase. These peaks become more pronounced when the film sintered at higher temperatures such as 700 °C.

Leakage current is a persistent challenge in KNN thin films due to the formation of conductive electron holes. It was proposed that the electron holes form due to oxidation of the films, enabled by the presence of oxygen vacancies which originate from loss of alkali oxides at the film surface during fabrication. Figure 4 illustrated variations in the current density J as a function of applied electric field E of 380 nm-thick Pt/KNN/Pt/SiO₂/Si capacitors. The J – E characteristic is considerably asymmetric with respect to voltage polarity. The leakage current with Pt electrode under a positive bias field is a bit noisier than that under a negative bias field. The noise often appears around 150 kV/cm. The cause of the noise disturbed in the positive electric field side is unknown. However, it is well-known that the leakage current was limited by the interface between electrode (top and bottom) and the film. Therefore, the electrical quality is better at the bottom-interface than that of current density at the top-interface. The asymmetric J – E curves may be associated with the different quality of Pt for top and bottom electrodes. The lowest value of leakage current density for KNN films is obtained around $3.85 \times 10^{-8} \text{ A/cm}^2$ at -60 kV/cm. This value for our KNN thin films is remarkably lower than that of current density in the reported KNN-based films [19–21].

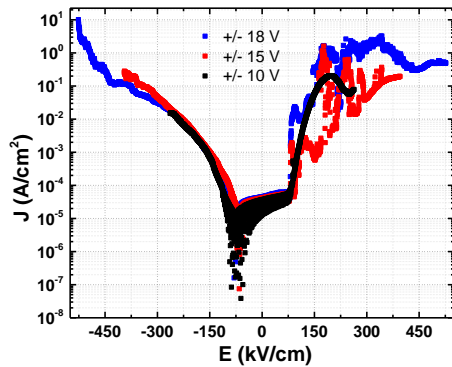


Figure 4. Leakage current density as a function of applied electric field of KNN thin film annealed at 650 °C.

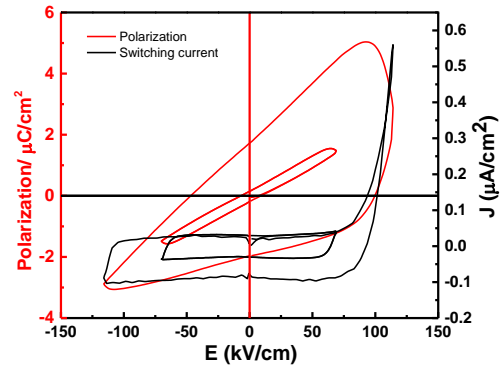


Figure 5. P-E hysteresis loop of the KNN film performed at 1 kHz (red curves) and its corresponding current flow (black curves).

In final, the ferroelectric nature of prepared KNN thin films was evaluated by a hysteresis loop of polarisation (P) as a function of an applied electric field (E) at 1 kHz, as shown in Figure 5. The corresponding current flow for these measurements was presented by the black curves in the same figure. Ferroelectric response obtained for KNN thin films was paraelectric-like at low bias voltages. It is worth to note that KNN thin films could not be withstood higher applied fields above 150 kV/cm as in the J–E measurements, and showed larger ferroelectricity, indicating that the film contains some leakage components. Hence, there is no switching current peaks that is often observed due to the polarisation reversal, but a strong current increase is found at higher electric field. Obviously, the presence of a leakage current strongly affects both remnant polarization and coercive field. As shown in Figure 5, remnant polarization and coercive field increase in the P–E curves that is of course a nonphysical interpretation owing to leakage current superposed the displacement current [22]. We would like to emphasize that the P–E measurement is much more sensitive with leakage current through the KNN-capacitor structure. Takana *et al.* reported a similar electrical property change using (Na,K)-excess solutions [10]. To obtain the saturated P–E loops reported by Cho and Grishin, single phase, highly c-axis oriented KNN thin films, and has the traces of a superlattice structure are demanded [23]. The collinearity of the direction of the vertical capacitor and the polar axis, along which the multiple cells of KNN film growth contribute to the improving ferroelectricity. One of reasons for the very low ferroelectricity in our films (Figure 5, red curves) could be attributed to the absence of ferroelectric domains which are caused by alkaline poor potassium niobates, $K_4Nb_6O_{17}$.

4. Conclusion

In summary, we have successfully prepared $(Na_{0.5}K_{0.5})NbO_3$ (KNN) thin films on Pt/Ti/SiO₂/Si(100) substrates from precursor solutions by the sol–gel process. The perovskite phase of thin films forms at 650 °C. The thin films are smooth and crack-free. Na and K elements were volatilized during the heat treatment and the composition of the thin films was changed. The (Na,K)-excess precursor solutions are effective in compensating an A-site vacancy. The KNN thin film grown using 20 mol% K and Na excess precursor solutions, shows a relatively low leakage current density (3.85×10^{-8} A/cm² at -60 kV/cm) but still leaky shaped ferroelectric P–E hysteresis loop due to the existence of secondary phase (the effect of surplus alkaline ions on conduction). The optimum Na/K ratio would depend on the heat-treatment

conditions such as annealing temperature, keeping time, and heating rate. Thus, finding an appropriate excess of alkaline is a key role in achieving good KNN thin films.

Acknowledgments

The authors acknowledge the financial support of Hanoi University of Science and Technology, Grant No. T2018-PC-071.

References

- [1] S. Gupta, D. Maurya, Y. Yan, S. Priya, Chapter 3: Development of KNN-Based Piezoelectric Materials, in: S. Priya, S. Nahm (Eds.), Springer, New York, NY, 2012: pp. 89–119.
- [2] A. Safari, M. Hejazi, Chapter 5: Lead-Free KNN-Based Piezoelectric Materials, in: S. Priya, S. Nahm (Eds.), Springer, New York, NY, 2012: pp. 139–176.
- [3] X. Wang, U. Helmersson, S. Olafsson, S. Rudner, L. Wernlund, S. Gevorgian, Growth and field dependent dielectric properties of epitaxial $\text{Na}_{0.5}\text{K}_{0.5}\text{NbO}_3$ thin films, *Appl. Phys. Lett.* 73 (1998) 927–929.
- [4] M. Blomqvist, S. Khartsev, A. Grishin, A. Petraru, C. Buchal, M. Blomqvist, et al., Optical waveguiding in magnetron-sputtered $\text{Na}_{0.5}\text{K}_{0.5}\text{NbO}_3$ thin films on sapphire substrates, *Appl. Phys. Lett.* 82 (2003) 439–441.
- [5] C.W. Ahn, E.D. Jeong, S.Y. Lee, H.J. Lee, S.H. Kang, I.W. Kim, Enhanced ferroelectric properties of LiNbO_3 substituted $\text{Na}_{0.5}\text{K}_{0.5}\text{NbO}_3$ lead-free thin films grown by chemical solution deposition, *Appl. Phys. Lett.* 93 (2008) 212905.
- [6] A. Khan, Z. Abas, H. Soo Kim, I.-K. Oh, Piezoelectric thin films: an integrated review of transducers and energy harvesting, *Smart Mater. Struct.* 25 (2016) 053002.
- [7] F. Söderlind, P.-O. Käll, U. Helmersson, Sol–gel synthesis and characterization of $\text{Na}_{0.5}\text{K}_{0.5}\text{NbO}_3$ thin films, *J. Cryst. Growth.* 281 (2005) 468–474.
- [8] K. Tanaka, K. Kakimoto, H. Ohsato, Fabrication of highly oriented lead-free (Na, K) NbO_3 thin films at low temperature by Sol–Gel process, *J CRYST GROWTH.* 294 (2006) 209–213.
- [9] Y. Nakashima, W. Sakamoto, T. Shimura, T. Yogo, Chemical Processing and Characterization of Ferroelectric (K,Na) NbO_3 Thin Films, *Jpn. J. Appl. Phys.* 46 (2007) 6971–6975.
- [10] K. Tanaka, H. Hayashi, K. Kakimoto, H. Ohsato, T. Iijima, Effect of (Na, K)-Excess Precursor Solutions on Alkoxy-Derived (Na, K) NbO_3 Powders and Thin Films, *Jpn. J. Appl. Phys.* 46 (2007) 6964–6970.
- [11] H. Kungl, M.J. Hoffmann, Influence of Alkaline and Niobium Excess on Sintering and Microstructure of Sodium-Potassium Niobate ($\text{K}_{0.5}\text{Na}_{0.5}$) NbO_3 , *J Am. Ceram. Soc.* 93 (2010) 1270–1281.
- [12] X. Yan, W. Ren, X. Wu, P. Shi, X. Yao, Lead-free (K, Na) NbO_3 ferroelectric thin films: Preparation, structure and electrical properties, *J. Alloy. Compd.* 508 (2010) 129–132.
- [13] Y. Nakashima, W. Sakamoto, H. Maiwa, T. Shimura, T. Yogo, Lead-Free Piezoelectric (K,Na) NbO_3 Thin Films Derived from Metal Alkoxide Precursors, *JPN J APPL PHYS.* 46 (2007) 311–313.
- [14] C.W. Ahn, H.-I. Hwang, K.S. Lee, B.M. Jin, S. Park, G. Park, et al., Raman Spectra Study of $\text{K}_{0.5}\text{Na}_{0.5}\text{NbO}_3$ Ferroelectric Thin Films, *Jpn. J. Appl. Phys.* 095801 (2010) 09580.
- [15] M.M.S. Hamim, T.I.S. Ā, K.O. Hi, High Pressure Raman Study of KNbO_3 – KTaO_3 and KNbO_3 – NaNbO_3 Mixed Crystals, *J. Phys. Soc. Jpn.* 72 (2003) 551–555.
- [16] H. Search, C. Journals, A. Contact, M. Iopscience, I.P. Address, Raman Scattering Study of Piezoelectric ($\text{Na}_{0.5}\text{K}_{0.5}$) NbO_3 - LiNbO_3 Ceramics, *Jpn. J. Appl. Phys.* 46 (2005) 7064–7067.
- [17] H.J. Trodahl, N. Klein, D. Damjanovic, N. Setter, B. Ludbrook, D. Rytz, et al., Raman spectroscopy of (K,Na) NbO_3 and (K,Na) $1 - x\text{Li}_x\text{NbO}_3$, *Appl. Phys. Lett.* 93 (2015) 262901.
- [18] J. Liu, X. Li, Y. Li, Synthesis and characterization of nanocrystalline niobates, *J. Cryst. Growth.* 247 (2003) 419–424.
- [19] C.W. Ahn, S.Y. Lee, H.J. Lee, A. Ullah, J.S. Bae, E.D. Jeong, et al., The effect of K and Na excess on the ferroelectric and piezoelectric properties of $\text{K}_{0.5}\text{Na}_{0.5}\text{NbO}_3$ thin films, *J Phys D Appl Phys.* 42 (2009) 215304.

- [20] M. Abazari, A. Safari, Effects of doping on ferroelectric properties and leakage current behavior of KNN-LT-LS thin films on SrTiO₃ substrate, *J. Appl. Phys.* 105 (2009) 094101.
- [21] M. Abazari, A. Safari, Effect of manganese doping on remnant polarization and leakage current in K_{0.44}Na_{0.52}Li_{0.04}(Nb_{0.84}Ta_{0.10}Sb_{0.06})O₃ epitaxial thin films on SrTiO₃, *J. Appl. Phys.* 92 (2008) 212903.
- [22] K. Prume, T. Schmitz, S. Tiedke, Dynamic leakage current compensation in ferroelectric thin-film capacitor structures, *Appl. Phys. Lett.* 86 (2005) 142907.
- [23] C. Cho, A. Grishin, C. Cho, A. Grishin, Background oxygen effects on pulsed laser deposited Na_{0.5}K_{0.5}NbO₃ films: From superparaelectric state to ferroelectricity, *Appl. Phys. Lett.* 87 (2000) 4439–4448.